Neurosci. Bull. June, 2021, 37(6):763–776
https://doi.org/10.1007/s12264-021-00650-7

www.neurosci.cn
www.springer.com/12264

ORIGINAL ARTICLE

Mapping Domain- and Age-Specific Functional Brain Activity for Children's Cognitive and Affective Development

Lei Hao[1,2,3] · Lei Li[4] · Menglu Chen[1,3] · Jiahua Xu[1,3] · Min Jiang[1,3] · Yanpei Wang[1,3] · Linhua Jiang[4] · Xu Chen[5,6] · Jiang Qiu[5,6] · Shuping Tan[7] · Jia-Hong Gao[8] · Yong He[1,3] · Sha Tao[1] · Qi Dong[1] · Shaozheng Qin[1,3]

Received: 9 June 2020 / Accepted: 25 September 2020 / Published online: 20 March 2021

Abstract The human brain undergoes rapid development during childhood, with significant improvement in a wide spectrum of cognitive and affective functions. Mapping domain- and age-specific brain activity patterns has important implications for characterizing the development of children's cognitive and affective functions. The current mainstay of brain templates is primarily derived from structural magnetic resonance imaging (MRI), and thus is not ideal for mapping children's cognitive and affective brain development. By integrating task-dependent functional MRI data from a large sample of 250 children (aged 7 to 12) across multiple domains and the latest easy-to-use and transparent preprocessing workflow, we here created a set of age-specific brain functional activity maps across four domains: attention, executive function, emotion, and risky decision-making. Moreover, we developed a toolbox named Developmental Brain Functional Activity maps across multiple domains that enables researchers to visualize and download domain- and age-specific brain activity maps for various needs. This toolbox and maps have been released on the Neuroimaging Informatics Tools and Resources Clearinghouse website (http://www.nitrc.org/projects/dbfa). Our study provides domain- and age-specific brain activity maps for future developmental neuroimaging studies in both healthy and clinical populations.

Keywords Brain activity maps · FMRI · Cognition · Emotion · Reward · Development

Lei Hao, Lei Li and Menglu Chen have contributed equally to this work.

Supplementary Information The online version contains supplementary material available at https://doi.org/10.1007/s12264-021-00650-7.

✉ Sha Tao
taosha@bnu.edu.cn

✉ Shaozheng Qin
szqin@bnu.edu.cn

1 State Key Laboratory of Cognitive Neuroscience and Learning & IDG/McGovern Institute for Brain Research, Beijing Normal University, Beijing 100875, China

2 College of Teacher Education, Southwest University, Chongqing 400715, China

3 Key Laboratory of Beijing Key Laboratory of Brain Imaging and Connectomics, Beijing Normal University, Beijing 100875, China

4 School of Information Engineering, Huzhou University, Huzhou 313000, China

5 Key Laboratory of Cognition and Personality (SWU), Ministry of Education, Chongqing 400715, China

6 Faculty of Psychology, Southwest University, Chongqing 400715, China

7 Beijing HuiLongGuan Hospital, Peking University, Beijing 100096, China

8 Center for MRI Research, Academy for Advanced Interdisciplinary Studies, Peking University, Beijing 100871, China

Introduction

During childhood, the brain undergoes rapid and protracted development, along with increasingly improved competence in a wide range of cognitive and affective functions, including attention, memory, emotion, and reward [1]. Such improvement at the behavioral level is often accompanied by rapid development of the brain, with substantial changes in structure and function such as gray matter volume [2], cortical thickness [3], and functional activation intensity [4], as well as the structural and functional connectivity of large-scale networks [5, 6]. Moreover, there are both linear and non-linear age-related changes in brain structure and function at both regional and large-scale network levels [7, 8]. And different brain regions and systems exhibit highly heterogeneous patterns over development, some maturing earlier than others. These developmental features, with concomitant changes along multiple dimensions, pose challenges to map how each of them and their interplay unfolds as the brain matures, and even more challenging to determine the development of structure-function coupling and the principles of how brain maturation gives rise to increasing improvements in children's cognitive and affective competencies [3, 9]. Therefore, a systematic approach spanning a wide range of ages and multiple task domains is required to better assess the normative maturation of functional brain systems and networks. In the field of developmental cognitive neuroscience, mapping domain- and age-specific brain activity patterns is one critical step towards characterizing the normative neuronal development of children's cognitive and affective functions [2, 5, 10, 11]. This will also provide ample opportunities for further brain-inspired applications in the fields of education, mental health, and the diagnosis of children with neurodevelopmental disorders [12–14].

Recent advances in developmental neuroimaging techniques, especially non-invasive multimodal magnetic resonance imaging (MRI), offer an unprecedented opportunity to map brain maturation *in vivo* as well as typical and atypical neurodevelopment of children's cognition, emotion, and behavior [2, 5, 6, 10, 15–19]. In the past two decades, for instance, several influential national projects focusing on brain development in children and adolescents have been launched in the USA and Europe, such as the Philadelphia Neurodevelopmental Cohort [20], the Adolescent Brain Development study [21], and the IMAGEN project [22]. The typical research framework consists of normalizing individual brain images into a common or standard stereotactic space using a prior structural template, such as the International Consortium for Brain Mapping (ICBM152) templates [23]. Given that the brain undergoes rapid and protracted development during childhood, brain templates specific for young children have often been generated for MRI investigations in the pediatric population [24–28]. Recent studies have demonstrated several major benefits of using age-specific brain templates for pediatric participants, including fewer requirements for spatial deformation during image normalization and maintaining a great number of the pediatric characteristics of individual brains [24, 25, 29]. Therefore, creating domain- and age-specific functional activity maps is necessary for mapping the neurodevelopment of children's cognitive and affective functions.

The construction of functional activity templates for the pediatric brain requires the consideration of several major factors, including age differences and the heterogeneous development of different cognitive and affective domains. First, there are prominent age-related developmental changes in both brain structure and function which vary greatly across different regions [3, 26, 28, 30]. Numerous developmental neuroimaging studies, for instance, have demonstrated that unimodal areas such as the visual and sensorimotor cortices mature earlier than polymodal association areas, followed by higher-order prefrontal regions [31]. Second, the cognitive and affective functions of children are characterized by increasingly improved competence in a wide range of domains, including attention, executive function, emotion, and reward [5, 17, 32–34]. Decades of research in developmental psychology have characterized the heterogeneous development of children's cognitive and affective functions [35–39]. For instance, executive functions such as working memory undergo protracted development with much slower maturation than attention abilities [40], and emotional perception and incentive seeking mature earlier than higher-order cognitive control and emotion regulation [41]. Thus, a systematic approach to age-related changes in brain, cognition, and behavior across multiple task domains is required for the construction of functional activity maps.

In the present study, we aimed to construct a set of high-quality domain- and age-specific functional activity maps of the brain by integrating structural MRI and task-dependent fMRI across multiple domains in a large sample of typically developing children (n = 250, from 7 to 12 years old). High-quality structural and functional imaging data were collected on a 3T Siemens Prisma scanner. Children underwent fMRI while performing a set of four cognitive and affective tasks with well-established paradigms: attention network task, numerical n-back working memory, emotion perception, and risky decision making with reward (see Methods). We implemented the latest easy-to-use and transparent preprocessing workflow named fMRIPrep [42] to pre-process task-dependent fMRI data and constructed a general linear model (GLM) for different age groups with multiple domains. Multiple linear

regression was used to estimate overall age-related brain maps. More importantly, we developed a Python-based toolbox named Developmental Brain Functional Activity (DBFA) mapping that provides an instrument with convenient access to domain- and age-specific brain activity maps (Fig. 1C). The public availability of this toolbox with functional brain activity maps will provide ample opportunities and potential for applications to mapping the typical and atypical neurodevelopment of children's cognitive and affective functions, and among other domains in both healthy and clinical populations.

Methods and Materials

Participants

We examined a large sample of 250 typically developing children from 7 to 12 years old (mean = 9.21 ± 1.36) with 4 cognitive tasks, which was derived from the Children School Functions and Brain Development Project (CBD, Beijing Cohort). The attention task (attention network test, ANT) included 240 participants, the executive function task (numerical n-back working memory, WM) included 245, the emotion task (emotion matching, EM) included 249, and the risky decision-making task (balloon analogue risk task, BART) included 250. The number of participants in the toolbox of these functional activity maps will be continuously updated as the project progresses. All participants reported no history of vision problems, no history of neurological or psychiatric disorders, and no current use of any medication or recreational drugs. Written informed consent was given by each child and one of their parents or legal guardians. The procedures of consent and experiment were approved by the local Ethics Committee and were in accordance with the standards of the Declaration of Helsinki. The inclusion criteria of head motion by mean frame-wise displacement (FD) was <0.5 mm in each task. The demographics of the dataset for 4 tasks are listed in Table S1.

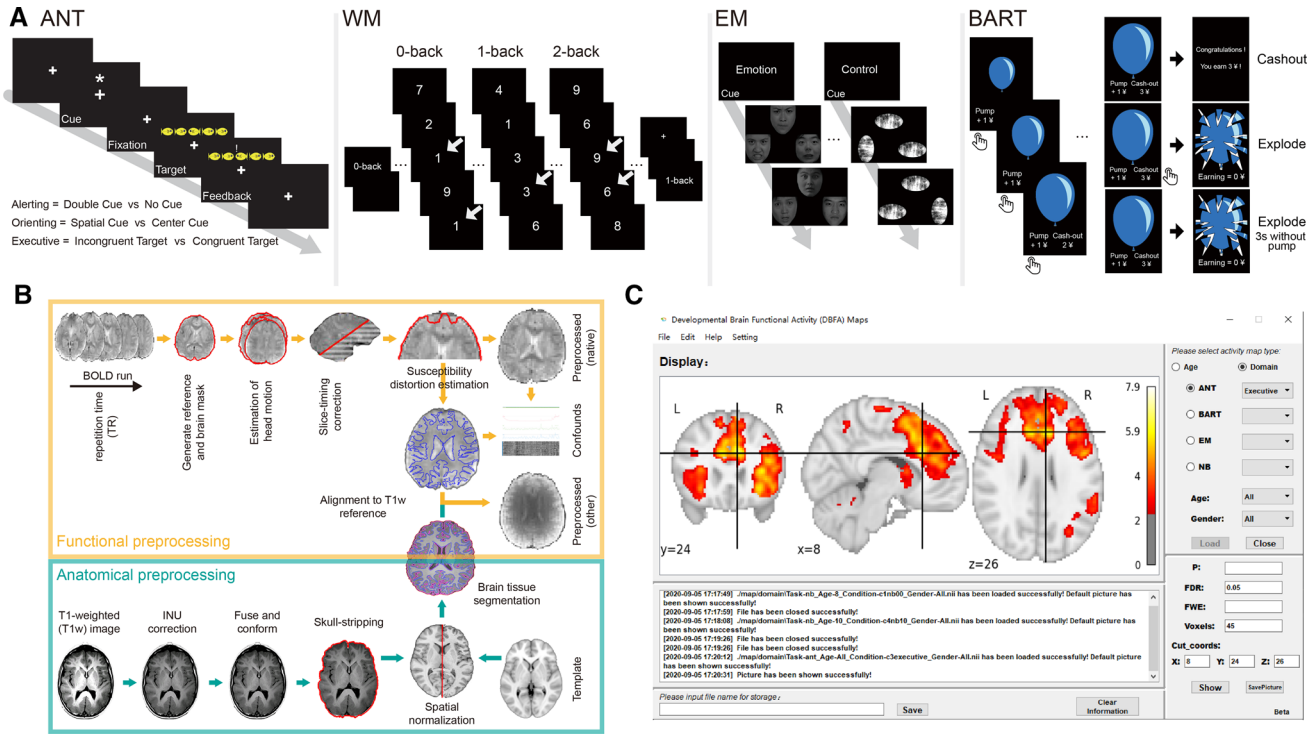

Fig. 1 Task designs, preprocessing workflow, and the main interface of the developmental brain functional activity (DBFA) toolbox. **A** Task designs for the four domains of attention, working memory, emotion, and reward risky decision-making. **B** Workflow of data preprocessing by fMRIPrep [42]. Technical details of critical processing steps: (1) skull stripping, (2) BOLD reference image estimation, (3) head-motion estimation, (4) slice-timing correction, (5) susceptibility distortion correction (SDC), (6) registration, and (7) resampling BOLD runs onto standard spaces (spatial normalization). C The main interface of the DBFA toolbox with a set of core functions in the menu to visualize and download domain- and age-specific (with gender factor only for emotion processing) activity maps. Users can customize the threshold criteria in terms of *P* values and cluster-size of voxels, with uncorrected, false discovery rate (FDR), and familywise error (FWE) correction for multiple comparisons. Note: BOLD, blood oxygen level dependent.

Cognitive and Affective Tasks

Attention Network Test (ANT)

We opted for a child-friendly version of the ANT consisting of six conditions: four cue conditions and two target conditions [32, 43] (Fig. 1A). Each trial consisted of a target stimulus preceded by one of the four cue conditions (1) no-cue, (2) double-cue, (3) center-cue, or (4) spatial-cue, either above or below the fixation cross at the screen center. The centrally presented target 'fish' was flanked by one of the three different types of 'fish' stimulus: (1) congruent flanker 'fish', (2) incongruent flanker 'fish', or (3) only a 'fish'. Each trial started with a fixation cross at the central of the screen for 400 ms to 1000 ms. Thereafter, in some of the next trials a warning cue appeared for 150 ms. And a stationary fixation phase of 450 ms was presented after the end of the cue. Thereafter, the target 'fish' stimulus with one of two types of flanker (congruent or incongruent) was presented until the participant made a button press or reached the time limit of 1000 ms. The duration of the last fixation was 1000 ms minus the corresponding reaction time. After responding, the participant received visual feedback from the computer. For correct responses, a simple animation sequence showed the target fish blowing bubbles. Incorrect responses had no animation of the fish. In each trial, the participant had to press either a left or right button indicating the direction of the centrally-presented arrow in the target phase. Participants were instructed to make a decision response as quickly and accurately as possible in each trial. The entire task was divided into two runs, each of which lasted $\sim$6 min. Stimuli were presented *via* E-Prime 2.0, which is widely used in psychological experiments (http://www.pstnet.com; Psychology Software Tools, Inc., Pittsburgh, PA).

Numerical n-Back Working Memory (WM)

A classic numerical n-back task was used to assess WM (Fig. 1A). Participants completed 12 cycles of three workloads (0-, 1-, and 2-back) by a jittered resting-fixation baseline ranging from 8 s to 12 s. Within each block, a random sequence of 15 single digits was shown to the participant. Each digit was presented for 400 ms, followed by an inter-stimulus interval of 1400 ms. Each block lasted 27 s. During the 0-back condition, the participant was asked to detect whether the current item on the screen was a "1" or not. During the1-back condition, the participant was asked to respond to the current item the same as the last one; and in the 2-back condition, the participant was asked to detect whether the current item had appeared two positions back in the sequence. Each participant was instructed to press a button with the index finger when detecting a target. Stimuli were presented *via* E-Prime 2.0.

Emotion Matching (EM)

The emotional processing task with a randomized block-design was adapted from a widely-used paradigm designed by Hariri and colleagues [44] (Fig. 1A). This task consisted of two conditions of both emotional and sensorimotor control blocks. During the emotional block, each participant viewed a trio of emotional faces, and was instructed to select one of two faces below that expressed the same category of emotion (anger/fear) as the target face above. During the sensorimotor control block, each participant viewed another trio of mosaic geometric shapes (circles, vertical and horizontal ellipses) filled by scrambled faces, and was asked to select one of two shapes below that was identical to the target shape above. Each block started with a cue for 5 s indicating either the emotional or control condition, followed by six trios of images presented sequentially for 5 s each. Stimuli were presented *via* E-Prime 2.0.

Balloon Analogue Risk Task (BART)

A modified version of the BART [45] with an event-related design was used to map task-invoked brain activity patterns involved in the reward and/or incentive domain. The BART consisted of three conditions: pump, cash-out, and explode, pending each participant's decision choice (Fig. 1A). During the task, each participant was shown a virtual balloon and given the option to inflate it by pressing the 'pump' button, or to stop by pressing the 'cash-out' button within 3000 ms. Otherwise, the balloon would explode automatically if there was no response. Each participant accumulated monetary rewards in a temporary bank with each pump (1 ¥ per pump), which could be transferred to a permanent bank by making the 'cash-out' decision. The balloon could explode at any moment after a 'pump' choice, indicating that the money accumulated in the temporary bank would be lost. Therefore, each trial of this task started with the presentation of a computerized balloon and came to an end when the balloon either exploded or the participant decided to cash-out. The number of trials completed during this self-paced task was not predetermined but depended on each participant's decisive response speed. Stimuli were presented *via* E-Prime 2.0.

Imaging Data Acquisition

Whole-brain images from each participant were acquired using the same type of Siemens 3.0T scanner (Magnetom

Prisma syngo MR D13D, Erlangen, Germany) at two sites with a 64-channel head coil and a T2*-sensitive echo-planar imaging (EPI) sequence based on blood oxygenation level-dependent contrast. Thirty-three axial slices (3.5 mm thick, 0.7 mm skip) parallel to the anterior and posterior commissural line and covering the whole brain were imaged with the following parameters: repetition time (TR) = 2000 ms, echo time (TE) = 30 ms, flip angle = 90°; voxel size = 3.5 × 3.5 × 3.5 mm^3, and field of view (FOV) = 224 × 224 mm^2. In addition, high-resolution anatomical images from each participant were acquired by three-dimensional sagittal T1-weighted magnetization-prepared rapid gradient echo (MPRAGE) with a total of 192 slices (TR = 2530 ms, TE = 2.98 ms, flip angle = 7°, inversion time = 1100ms, voxel size = 1.0 × 1.0 × 1.0 mm^3, acquisition matrix = 256 × 224, FOV = 256 × 224 mm^2, brand width = 240 Hz/Px, slice thickness = 1 mm). The order of the four tasks was fixed for all participants: EM, WM, ANT, and BART. The interval between tasks was 2–5 min, depending on whether participants felt that they had enough rest between tasks. A potential order effect would not affect task- and age-specific brain activity maps in the present study; it would be of particular concern when directly comparing activity patterns between different tasks. It was not the case in the present study, because we had no intention nor hypotheses to compare activity maps between tasks. For the ANT task, the number of volumes was 177, lasting 354 s; for the WM task 232 volumes and 462 s; for the EM task 179 volumes and 359 s; and for the BART task 184 and 368 s.

Pre-processing of fMRI Data

Brain images were preprocessed using fMRIPrep 1.4.1 (RRID:SCR_016216) [42], which is based on Nipype 1.2.0 (RRID:SCR_002502) [46]. Specifically, the first 4 volumes of each run for all tasks were discarded for signal equilibrium and the adaptation of participants to scanning noise. For each run per participant (across all tasks and sessions), the following preprocessing was performed. First, a reference volume and its skull-stripped version were generated using a custom methodology of fMRIPrep. Co-registration was configured with nine degrees of freedom to account for distortions remaining in the BOLD reference. Head-motion parameters with respect to the BOLD reference (transformation matrices and six corresponding rotation and translation parameters) were estimated before any spatiotemporal filtering using mcflirt (FSL 5.0.9). Functional images of each task were slice-time corrected using 3dTshift from AFNI. The resultant images (including slice-timing correction when applied) were resampled into their original, native space by applying a single composite transformation to correct for head-motion and susceptibility distortions. These resampled images are referred to as preprocessed BOLD functional images in the original space. After that, images were resampled into a standard space, generating a preprocessed BOLD run in the well-known 'MNI152NLin6Asym' space. More details are provided in the Supplementary Methods.

Motion artifacts were automatically removed using independent component analysis (ICA-AROMA) of the preprocessed images in MNI space time-series after removal of non-steady-state volumes and spatial smoothing with an isotropic, Gaussian kernel of 6 mm full-width half-maximum. The head-motion estimates calculated in the correction step were also placed in the corresponding confounds file. The confound time series derived from head-motion estimates and global signals were expanded with the inclusion of temporal derivatives and quadratic terms for each. Frames that exceeded a threshold of 0.5 mm FD or 1.5 standardized DVARS were annotated as motion outliers. All re-sampling was performed with a single interpolation step by composing all the pertinent transformations (i.e., head-motion transform matrices, susceptibility distortion correction when available, and co-registration to anatomical and output spaces). Gridded (volumetric) resampling was performed using antsApplyTransforms, configured with Lanczos interpolation to minimize the smoothing effects of other kernels. More details are provided in the Supplementary Methods.

In addition, technical details of critical processing steps include as follows: (1) Skull stripping: brain tissue segmentation (cortex and cerebellum) from the surrounding region (skull and non-brain area). (2) BOLD reference image estimation: this workflow estimates a reference image for a BOLD series. (3) Head-motion estimation: using the previously estimated reference scan in step (2) to estimate head-motion. As a result, one rigid-body transform with respect to the reference image is written for each BOLD time-step. (4) Slice-timing correction: a preprocessing step applied to correct for slice-dependent delays, achieved by shifting the time series of each slice to temporally align all slices to a reference time-point. All slices are realigned in time to the middle of each repetition time (TR). (5) Susceptibility distortion correction (SDC): one of the major problems that affects (EPI) data is the spatial distortion caused by the inhomogeneity of the field inside the scanner. (6) Registration: the alignment between the reference EPI image of each run and the reconstructed image of each participant using the gray/white matter boundary. (7) Resampling BOLD runs onto standard spaces (spatial normalization): a preprocessing step that involves deforming the brain image from each participant so that it fits a standardized (template) brain image, to remove global differences in the size and orientation of each 'normalized' brain and so that the same anatomical regions in each

image occupy the same voxels, with attendant reduced statistical variance and increased power. More details are provided in the Supplementary Methods.

Univariate General Linear Model (GLM)

To assess task-dependent brain responses in the ANT, WM, EM, and BART, we constructed a GLM with separate regressors corresponding to experimental conditions manipulated in each of the four task domains. For the ANT task, we modeled correct and incorrect trials separately. For the WM and EM tasks, we could not readily model correct and incorrect trials separately, because a blocked rather than event-related fMRI design was used. For the BART, there were no right or wrong trials, given that we used a classical risk-taking paradigm with each participant making self-choices. Instead, we modeled the three separate phases of each risk-taking action: pump, cash-out, and explode.

For the ANT, six conditions (no-cue, double-cue, center-cue, spatial-cue, congruent-target, and incongruent-target) were modeled as 6 separate event-related regressors. Relevant contrast parameter estimate images were initially generated at the individual-subject level, in the alerting (double-cue *vs* no-cue), orienting (spatial-cue *vs* center-cue), and executive (incongruent-target *vs* congruent-target) conditions, and were submitted to second-level group analysis.

For WM, three conditions (0-, 1- and 2-back) were modeled as separate regressors. Relevant contrast parameter estimate images were initially generated at the individual-subject level, in the 0-, 1- and 2-back conditions, and were submitted to second-level group analysis.

For EM, the emotional and sensorimotor control conditions were modeled as separate boxcar regressors. Relevant contrast parameter estimate images were initially generated at the individual-subject level, in 2 regressors (emotion and control blocks) and the emotion *vs* control condition, and were submitted to second-level group analysis. For this task, we also constructed a GLM for different conditions with all, as well as boys and girls separately.

For BART, three conditions (pump: making risky decisions; cash-out: receiving rewards; explode: experiencing risks) were modeled as three separate event-related regressors. Corresponding contrast parameter estimated images, were initially generated at the individual level in the pump, cash-out, explode conditions, and were submitted to second-level group analysis.

Each model of the four task domains was convolved with the canonical hemodynamic response function implemented in SPM12 (https://www.fil.ion.ucl.ac.uk/spm/software/spm12). In addition, two global signals extracted within the CSF and WM from each participant were included to regress out effects related to noise. We used high-pass filtering using a cutoff of 1/128 Hz, and corrections for serial correlations in fMRI using a first-order autoregressive model (AR (1)) in the GLM framework. One-sample *t*-tests were applied in the second-level group analysis for the four task domains to create a domain-specific pattern of functional activation. Significant clusters were determined using a stringent threshold of $P < 0.05$ (cluster size >45) false discovery rate correction for multiple comparisons.

Moreover, we used multiple linear regression to identify overall age-related activation maps in the whole-brain analyses, with age as a covariate of interest and other confounding factors (gender and site variables) as nuisances. For the ANT, WM, and BART domains, age was modeled as the covariate of interest, and gender and site variables as the confounding factors, to identify age-related changes in activation patterns. For the EM task, age was modeled as the covariate of interest and the site variable as a confounding factor to identify age-related changes in activation patterns in boys and girls. In addition, we calculated a set of simple comparisons by using independent sample *t*-tests between boys and girls in all three conditions (emotion, control, and emotion *vs* control) (see Supplementary Information).

DBFA Toolbox

Given that many tools and scripts used in the fields of neuroimaging and brain science are based on Python, we decided use Python to develop the DBFA toolbox in order to connect well with freely available resources. PyQt, a toolkit for creating graphical user interface (GUI) applications, is a successful fusion of Python programming language and the Qt library, which is one of the most powerful libraries at present. So we used PyQt5 + Eric6 + Python 3.7 as the compilation and development environment, and then imported three packages of the QtCore, QtGui, and QtWidgets to generate GUI component objects such as buttons, text boxes, display boxes, and combo boxes. Qt components reserved the slot function interfaces to load the required functions and realize the separation of interface and logic. After the GUI was completed, we imported functions of neuroimage packages such as nistats and nilearn (i.e., map_threshold, plot_stat_map, and new_img_like) to implement customized threshold criteria in terms of *P* values, the cluster-size of voxels, and the results presented. Finally, we chose Cx-Freeze as a packaging tool to generate the final executable program.

Several major functions were implemented in the DBFA toolbox: (1) user-customized domain- or age-specific brain functional activity maps; (2) user-customized task, age range, and gender of the activity maps desired to

download; (3) user-customized threshold criteria in terms of *P* values and cluster-size of voxels, with a set of options including uncorrected, false discovery rate, and familywise error correction for multiple comparisons; (4) user-customized coordinates of any brain regions desired to display; and (5) user-customized local path to host brain activity maps with different threshold criteria.

Results

Domain- and Age-Specific Brain Activity Patterns Involved in Three Core Attention Processes

First, we created domain-specific brain activity maps associated with ANT, including alerting, orienting, and executive control. As shown in Fig. 2A, we found prominently significant clusters in a set of widely distributed regions in the occipital, dorsal attention, ventral attention, and cingulo-opercular systems involved in three core attention processes in children from 7 years to 12 years old. Specifically, for alerting, we found prominent clusters in the lateral occipital, superior parietal lobule (SPL), frontal eye fields (FEF), and ventral frontal cortex (VFC). For orienting, we found prominent clusters in the temporo-parietal junction, SPL, FEF, VFC, and supplementary motor area (SMA). For executive attention, we found prominent clusters in the dorsal anterior cingulate cortex (dACC), anterior insula (AI), FEF, and VFC. We further created age-specific brain activity maps associated with the three attention processes in each age group in children from 7 years to 12 years old at one-year intervals (11 years and 12 years old merged because of fewer participants). As shown in Fig. 2B, activation was an increasingly more pronounced as age increased from 7 years to 12 years in the brain systems associated with alerting (for all three conditions, see Fig. S1A).

In addition, we created age-related brain activity maps by using multiple regression analyses to show the relationship of task-invoked activation intensity with age. We found positive correlations in the SPL for alerting, negative correlations in the right FEF, right VFC, and left SMA for orienting, and positive correlations in the right dACC, AI, cuneus, and middle cingulate cortex for executive attention (Fig. S1B). We also examined whether there are any differences in head motion (mean FD) for participants at age 10 compared to either 7, 8, 9, 11, or 12. These analyses revealed no significant difference after Bonferroni multiple-comparison correction (Table S2).

Domain- and Age-Specific Brain Activity Patterns Involved in Executive Function Processing

We further created domain-specific brain activity maps associated with different WM loads. As shown in Fig. 3A, we found prominent clusters in a set of widely distributed regions in the occipital, fronto-parietal, and cingulo-opercular systems involved in distinct WM load (1- and

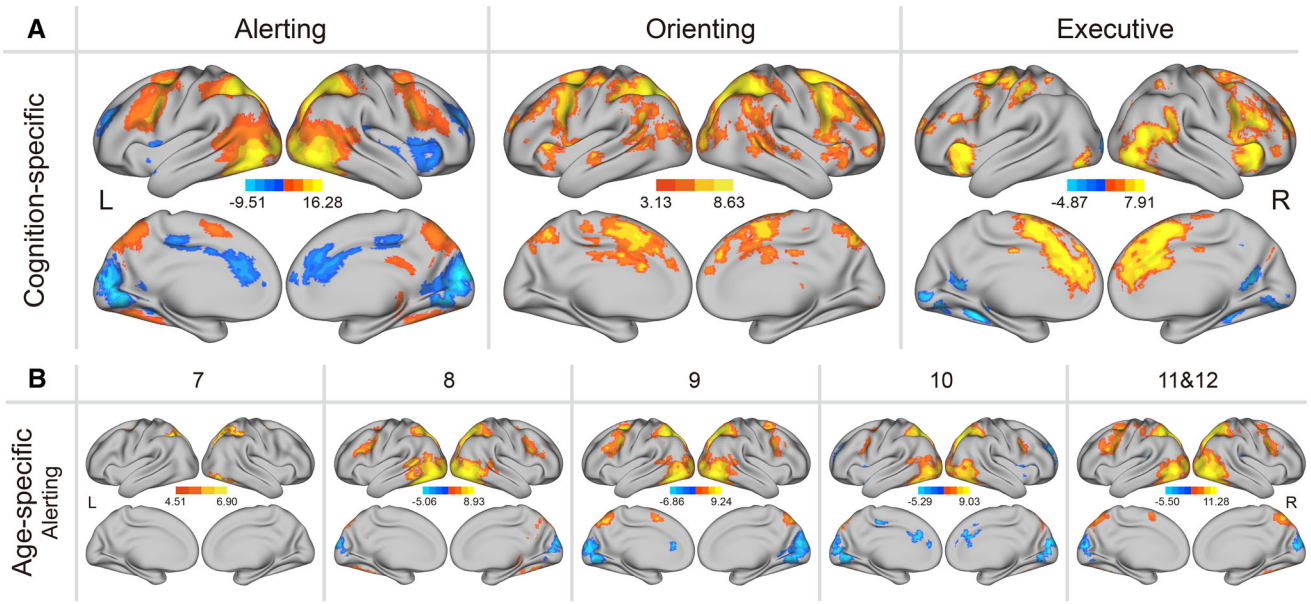

Fig. 2 Domain- and age-specific brain activity patterns for alerting, orienting, and executive attention in children. Significant clusters corresponding to three core attention processes superimposed onto a 2D brain surface space. **A** Domain-specific brain activity maps. Lateral and medial views of significant clusters in widespread brain regions for alerting, orienting, and executive attention. **B** Age-specific brain activity maps. Lateral and medial views of significant clusters in widespread brain regions in each age group for alerting attention (all three conditions are provided in Fig. S1A). Color bars indicate corresponding levels of *t* value.

2-back) processes in children from 7 years to 12 years old. Specifically, widespread brain activation in the frontal-parietal network, including the dorsal lateral prefrontal cortex (DLPFC), ventral lateral prefrontal cortex (VLPFC), rostral prefrontal cortex, inferior parietal lobule (IPL), angular gyrus, AI, caudate, and SMA, were involved in distinct WM load (1- and 2-back) processes in children from 7 years to 12 years old, but no activation in the IPL and right DLPFC was involved in 0-back. We also found the strength of brain activation in these regions increased with the increase of WM load. We further created age-specific brain activity maps associated with different WM loads in each age group in children from 7 to 12 years old at one-year intervals. As shown in Fig. 3B, we found increasingly more pronounced activation as age increased from 7 to 12 years in the brain systems associated with 2-back (for all three conditions, see Fig. S2A).

In addition, we created age-related brain activity maps by using multiple regression analyses to show the relationship of task-invoked activation intensity with age. We found positive correlations in the middle fontal gyrus and left VFC, and a negative correlation in the cuneus for the 0-back condition; a positive correlation in the left VFC and negative correlations in angular, cuneus, and hippocampus for the 1-back condition; and positive correlations in the DLPFC, SPL, SMA, and AI, and negative correlations in posterior insula, angular, cuneus, hippocampus, posterior cingulate cortex, and subgenual anterior cingulate cortex for the 2-back condition (Fig. S2B).

Domain- and Age-Specific Brain Activity Patterns Involved in Emotional Processing

We next created domain-specific activity maps associated with emotional processing, sensorimotor control, and emotion *vs* control conditions. As shown in Fig. 4A, we found widespread activation in the amygdala, insula, occipital, parietal, and ventral frontal cortices involved in those three conditions in children from 7 years to 12 years old. For all samples, and for boys and girls, we found prominent activation in the amygdala, thalamus, occipital, inferior parietal lobule, VFC, AI, and SMA for emotional processing and emotion *vs* control conditions, plus the FEF only in emotional processing; we found prominent activation in occipital, parietal, temporo-parietal junction (TPJ), postcentral gyrus, FEF, VFC, AI, and SMA for the sensorimotor control condition. We further created age-specific activity maps associated with the three conditions in each age group in children from 7 years to 12 years old at one-year intervals. As shown in Fig. 4B, we founded an increasingly more pronounced activation as age increased from 7 years to 12 years in the systems associated with emotional processing (for all three conditions see Fig. S3).

In addition, we created age-related brain activity maps by using multiple regression analyses to show the relationship of task-invoked activation intensity to age. We found positive correlations in the striatum and lateral occipital (LO), and negative correlations in the FEF, angular, precuneus, and middle cingulate cortex for

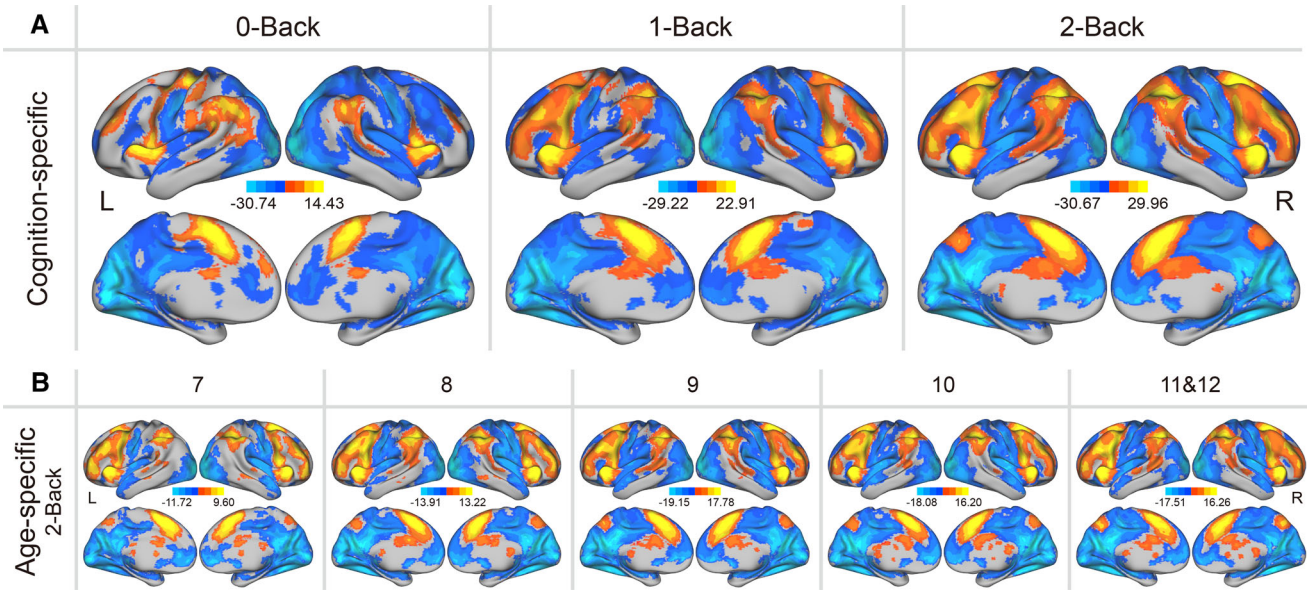

Fig. 3 Domain- and age-specific activity patterns for three working memory (WM) loads in children. Significant clusters corresponding to the different loads are superimposed onto a 2D brain surface space. **A** Domain-specific brain activity maps. Lateral and medial views of significant clusters in widespread brain regions associated with 0-, 1-, and 2-back WM tasks. **B** Age-specific brain activity maps. Lateral and medial views of significant clusters in widespread brain regions in each age group associated with the 2-back WM condition (all three conditions are provided in Fig. S2A). Color bars indicate corresponding levels of *t* value.

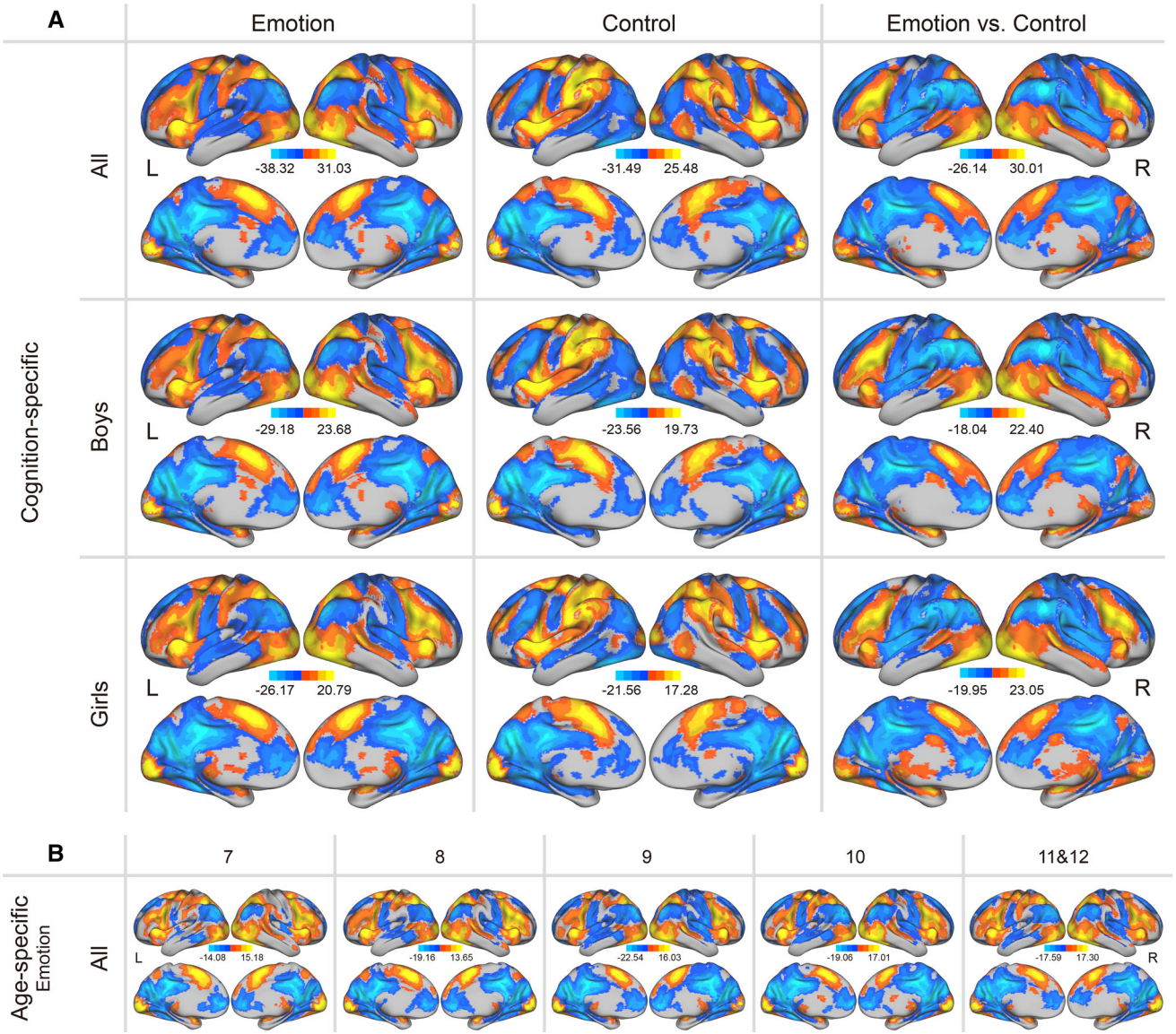

Fig. 4 Domain- and age-specific brain activity patterns for emotional processing in children. Significant clusters corresponding to emotional processing are superimposed onto a 2D brain surface space. **A** Domain-specific brain activity maps. Lateral and medial views of significant clusters in widespread regions associated with emotional processing, sensorimotor control, and emotion *vs* control conditions in all samples, and boys and girls separately. **B** Age-specific activity maps. Lateral and medial views of significant clusters in widespread regions in each age group associated with emotional processing conditions in all samples (all conditions are provided in Fig. S3). Color bars indicate corresponding levels of *t* value.

emotional processing; positive correlations in the AI and SMA, and negative correlations in the angular and cuneus for sensorimotor control processing; and positive correlations in the SPL and LO, and negative correlations in the anterior middle frontal gyrus, SMA, TPJ, and right AI for emotion *vs* control conditions (Fig. S4). Independent sample *t* tests revealed that boys exhibited significantly higher activation in the subgenual anterior cingulate cortex (sgACC) for emotion and in the sgACC and precuneus for emotion *vs* control, as well as significantly lower activation in the LO for the control condition, when compared to girls (Fig. S6).

Domain- and Age-Specific Brain Activation Patterns Involved in Reward Decision-Making Processing

We next created domain-specific brain activity maps associated with different reward decision-making processing. As shown in Fig. 5A, we found prominent clusters in a set of widely distributed regions in the whole brain involved in the pump, cash-out, and explode processes in

children from 7 years to 12 years old. Specifically, for pump we found prominent clusters in the LO, IPL, TPJ, DLPFC, AI, striatum (caudate and putamen), and SMA. For cash-out, we found prominent clusters in the LO, IPL, TPJ, middle temporal gyrus (MTG), DLPFC, AI, and SMA. For explode, we found prominent clusters in the LO, IPL, TPJ, MTG, DLPFC, AI, and SMA. We further created age-specific activity maps associated with different reward decision-making processing in each age group of children from 7 years to 12 years old at one-year intervals. As shown in Fig. 5B, we found increasingly more pronounced activation as age increased from 7 years to 12 years in different brain systems associated with the pump process (for all three conditions see Fig. S5A).

Finally, we created age-related brain activity maps by using multiple regression analyses to show the relationship of task-evoked activation intensity with age. We found positive correlations in the SPL, VFC, SMA, striatum, right AI and negative correlations in the middle fontal cortex and left angular for the making risky decisions process; positive correlations in the AI, right DLPFC, right IPL, and TPJ, and negative correlations in the left angular and precuneus for the receiving rewards process; and positive correlations in the right DLPFC, right TPJ, and MTG, and negative correlations in anterior middle fontal gyrus and cuneus for the experiencing risk process (Fig. S5B).

Discussion

In the present study, we constructed a set of domain- and age-specific developmental functional activity maps from a pediatric population across four domains with multiple cognitive and affective tasks. By implementing the latest preprocessing pipeline, we found heterogeneous activity patterns in widely distributed systems involved in the four different domains attention, executive function, emotion perception, and risky reward decision-making. There were prominent age-related changes in task-invoked functional activation within widespread systems from 7 years to 12 years old. Moreover, we developed the DBFA toolbox to visualize and download these domain- and age-specific brain activity maps with customized and standard threshold criteria. This toolbox is publicly available from http://www.nitrc.org/projects/dbfa, which provides ample opportunities for future data-mining and advanced analyses to characterize the typical neurodevelopment of children's cognitive and affective functions.

Generally speaking, the distinct task-invoked activity patterns associated with the four domains in young children coincide with the theoretical framework of domain-specific systems involved in cognitive and affective functions [47, 48], suggesting the emergence of heterogeneous neurodevelopment of children's cognitive and affective functions as young as 7 years to 12 years old. Specifically, the activation patterns involved in alerting were primarily

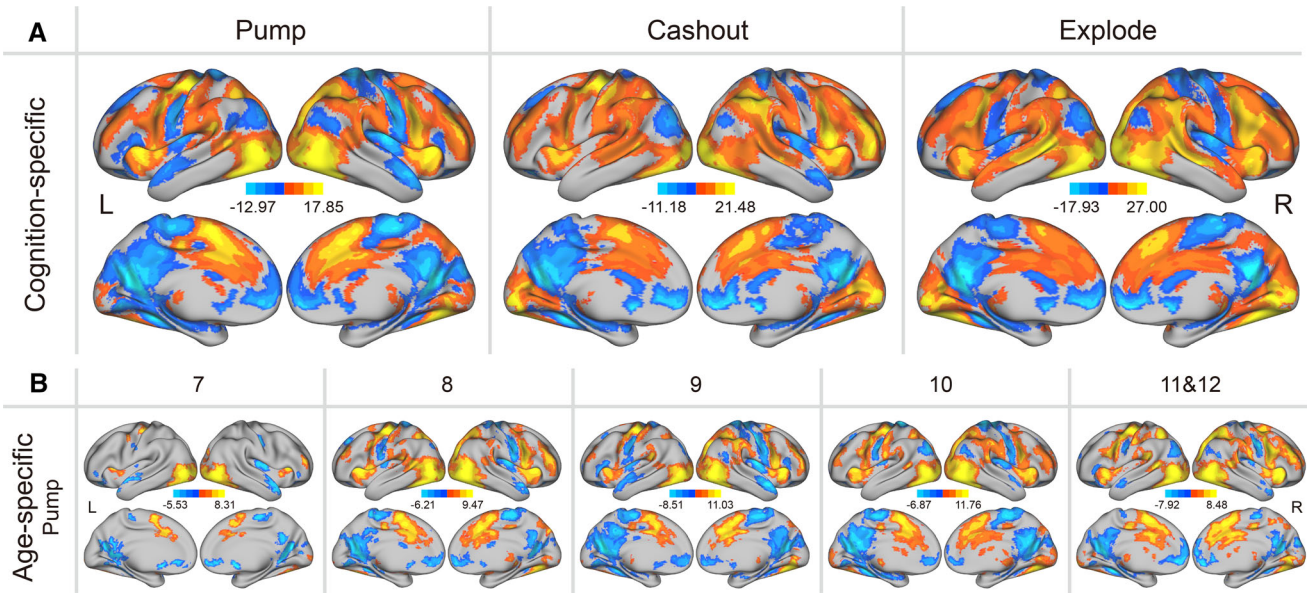

Fig. 5 Domain- and age-specific brain activity patterns for pump, cash-out, and explode processes in children. Significant clusters corresponding to different reward decision-making processing superimposed onto a 2D brain surface space. **A** Domain-specific activity maps. Lateral and medial views of significant clusters in widespread regions associated with making risky decisions (pump), receiving rewards (cash-out), and experiencing risks (explode). **B** Age-specific activity maps. Lateral and medial views of significant clusters in widespread regions in each age group associated with the pump condition (all conditions are provided in Fig. S5A). Color bars indicate corresponding levels of *t* value.

localized in the visual, ventral attention network, and motor systems, similar to previous findings in adults [49–53]. But we did not find significant cluster(s) in the thalamus in alerting like that reported in adults [49, 50]. The activation patterns involved in orienting were localized in the conventional dorsal attention network and motor systems, similar to previous findings in adults [49, 54]; and the activation patterns in executive attention were localized in the conventional cingulo-opercular and frontal-parietal networks, similar to previous findings in adults [49, 50]. We found that functional activation in the FEF for the alerting process exhibited an initial increase with age, and then a decrease at age 10. Such a non-linear developmental pattern of attention-related frontal function may reflect a developmental interplay of attentional processes and other cognitive abilities, such as reading in school-aged children, particularly during middle and late childhood [55–58]. Specifically, 9 years –10 years is the critical period of children's cognitive development, and many such abilities pertaining to attention (e.g., reading) [59–61] undergo dramatic changes in this age range [62–64]. It is worth noting that the decreased activation in alerting process at ages 9-10 cannot be readily explained by developmental changes in head motion, as we did not find significant differences in FD for children at 10 compared to 7, 8, 9, 11, or 12 year-olds. For working memory, the activation patterns were primarily localized in the conventional frontal-parietal network and among others, including the DLPFC, VLPFC, IPL in the1- and 2-back conditions, similar to previous findings in adults [65, 66]. For emotional processing, the activation patterns were primarily localized in the emotional and salience networks including the amygdala and AI, similar to previous findings in both adults and children [44, 67]. The differences between boys and girls in the emotion task demonstrated sex difference in the development of emotional reactivity to facial expressions [68]. Social emotional development theory posits that this difference most likely results from higher social awareness in girls than in boys during childhood [69]. Sex differences in emotional processing highlight the sex heterogeneity of emotion-related brain systems or networks during development, which has important implications for understanding the etiology of sex-specific interventions and treatments of emotion-related disorders. For reward or risky decision-making, the activation patterns were primarily localized in the striatum (caudate and putamen), AI, DLPFC, and anterior cingulate cortex, concurring with triadic neurocognitive models of reward-based risky behaviors consisting of the three components avoidance, approach, and executive control [70]. In addition, some activation patterns were less pronounced in young children than in adults. This discrepancy may be attributed to two major factors: application of the latest data preprocessing and the developmental nature of the pediatric population as discussed below. First, the development of systems and networks in the pediatric population becomes increasingly specialized toward nuanced cognitive and affective functions. The less pronounced activation patterns in children may explain relatively inferior performance of various cognitive abilities in children as compare to adults. Second, several studies have shown that different preprocessing methods may cause some differences in functional activity patterns [71–74]. Our work used a newly developed preprocessing pipeline named fMRIPrep [42, 75] for transparency and reproducibility purposes.

There are several major strengths and differences in our domain- and age-specific functional activity maps relative to other brain templates [24–28]. First, our functional activity maps consist of multiple task domains, which also goes beyond the mainstay of brain templates and activity maps derived from anatomical MRI data and single-task paradigms, respectively. Second, our activity maps are constructed by integrating task-dependent fMRI data with optimized signal-to-noise ratios in state-of-the-art 3.0-T Prisma scanners used worldwide in the most influential human brain projects, including the Human Connectome Project (HCP) and Adolescent Brain Cognitive Development (ABCD) [24, 25]. Third, our activity maps are derived from a large sample of 250 children from 7 to 12 years old, a phase of rapid and dynamic maturation which is important for obtaining repeatable and robust accurate descriptions of children's brains. Fourth, by using a toolbox named DBFA with the most commonly-used MNI-coordinate space, these activity maps are publicly available, which makes their application convenient and generalizable. The domain-specific functional brain activity maps that we constructed in this study open ample new opportunities for mapping children's cognitive and affective functions using pediatric neuroimaging techniques. Recent studies suggest that approximately half of the population fulfil the criteria for one or other psychiatric disorder, and most of those have onset ages in childhood or adolescence [13, 76, 77]. Constructing their neurodevelopmental activity maps is thus crucial for understanding children's typical and atypical neurodevelopment principles. These activity maps provide a set of comprehensive reference templates for future developmental neuroimaging studies in both healthy and clinical populations.

Converging findings from four different domains have important implications for understanding typical and atypical neurodevelopment of cognitive and affective functions. This not only provides domain- and age-specific brain functional activity maps and templates for future developmental neuroimaging studies, but also offers the potential to promote the development of brain-inspired

biomarkers for the detection of those with atypical neurodevelopment in certain domain(s). It is worth noting that there are several limitations in our present study. First, the functional activity maps were derived from a cross-sectional rather than a longitudinal design. Second, the age range in children was from 7 to 12, with no coverage over adolescence. Expanding the age span with a longitudinal design is required for mapping the developmental trajectories from childhood to adulthood. Third, the neurobiological mechanisms underlying the emergence of domain- and age-specific differences in brain activity maps remain elusive, and further studies are needed to address this question.

In conclusion, our study highlights the construction of domain- and age-specific functional activity maps across multiple domains in school-aged children from 7 years to 12 years old, based on the application of state-of-the-art neuroimaging techniques and sophisticated analytical approaches. The activity maps derived from a relatively large sample with the DBFA toolbox are publicly available for researchers, which may provide ample opportunities for developmental neuroimaging studies in both healthy and diseased conditions to characterize the typical and atypical neurodevelopment of cognitive and affective functions in the pediatric population.

Acknowledgements We thank the National Center for Protein Sciences at Peking University for assistance with MRI data acquisition. This work was supported by the National Natural Science Foundation of China (31522028, 71834002, 31530031, 81571056, 31521063, and 61775139), the Youth Science and Technology Innovation Program, Beijing Brain Initiative of Beijing Municipal Science and Technology Commission (Z181100001518003), the Open Research Fund of the State Key Laboratory of Cognitive Neuroscience and Learning (CNLZD1503 and CNLZD1703), and the Fundamental Research Funds for the Central Universities. We thank Professor Xi-Nian Zuo for comments and helpful discussions of this manuscript.

Conflict of interest The authors declare no competing financial interests.

References

1. Johnson MH. Functional brain development in humans. Nat Rev Neurosci 2001, 2: 475–483.
2. Giedd JN, Blumenthal J, Jeffries NO, Castellanos FX, Liu H, Zijdenbos A. Brain development during childhood and adolescence: a longitudinal MRI study. Nat Neurosci 1999, 2: 861–863.
3. Shaw P, Greenstein D, Lerch J, Clasen L, Lenroot R, Gogtay N, *et al.* Intellectual ability and cortical development in children and adolescents. Nature 2006, 440: 676–679.
4. Golarai G, Ghahremani DG, Whitfield-Gabrieli S, Reiss A, Eberhardt JL, Gabrieli JDE, *et al.* Differential development of high-level visual cortex correlates with category-specific recognition memory. Nat Neurosci 2007, 10: 512–522.
5. Baum GL, Ciric R, Roalf DR, Betzel RF, Moore TM, Shinohara RT, *et al.* Modular segregation of structural brain networks supports the development of executive function in youth. Curr Biol 2017, 27(1561–1572): e8.
6. Fair DA, Cohen AL, Power JD, Dosenbach NUF, Church JA, Miezin FM, *et al.* Functional brain networks develop from a "local to distributed" organization. PLoS Comput Biol 2009, 5: e1000381.
7. Dosenbach NUF, Nardos B, Cohen AL, Fair DA, Power JD, Church JA, *et al.* Prediction of individual brain maturity using fMRI. Science 2010, 329: 1358–1361.
8. Gogtay N, Giedd JN, Lusk L, Hayashi KM, Greenstein D, Vaituzis AC, *et al.* Dynamic mapping of human cortical development during childhood through early adulthood. Proc Natl Acad Sci U S A 2004, 101: 8174–8179.
9. Baum GL, Cui Z, Roalf DR, Ciric R, Betzel RF, Larsen B, *et al.* Development of structure–function coupling in human brain networks during youth. Proc Natl Acad Sci U S A 2020, 117: 771–778.
10. Foulkes L, Blakemore S-J. Studying individual differences in human adolescent brain development. Nat Neurosci 2018, 21: 315–323.
11. Lenroot RK, Giedd JN. Brain development in children and adolescents: Insights from anatomical magnetic resonance imaging. Neurosci Biobehav Rev 2006, 30: 718–729.
12. Hazlett HC, Gu H, Munsell BC, Kim SH, Styner M, Wolff JJ, *et al.* Early brain development in infants at high risk for autism spectrum disorder. Nature 2017, 542: 348–351.
13. Paus T, Keshavan M, Giedd JN. Why do many psychiatric disorders emerge during adolescence?. Nat Rev Neurosci 2008, 9: 947–957.
14. Xia Y, Lv D, Liang Y, Zhang H, Pei K, Shao R, *et al.* Abnormal brain structure and function in first-episode childhood-and adolescence-onset schizophrenia: Association with clinical symptoms. Neurosci Bull 2019, 35: 522–526.
15. Dobbing J, Sands J. Quantitative growth and development of human brain. Arch Dis Child 1973, 48: 757–767.
16. Giedd JN, Snell JW, Lange N, Rajapakse JC, Casey BJ, Kozuch PL, *et al.* Quantitative magnetic resonance imaging of human brain development: ages 4–18. Cereb Cortex 1996, 6: 551–559.
17. Qin S, Young CB, Supekar K, Uddin LQ, Menon V. Immature integration and segregation of emotion-related brain circuitry in young children. Proc Natl Acad Sci U S A 2012, 109: 7941–7946.
18. Zuo X-N, He Y, Betzel RF, Colcombe S, Sporns O, Milham MP. Human connectomics across the life span. Trends Cogn Sci 2017, 21: 32–45.
19. Wang Y, Xu Q, Zuo C, Zhao L, Hao L. Longitudinal changes of cerebellar thickness in autism spectrum disorder. Neurosci Lett 2020:134949.
20. Satterthwaite TD, Connolly JJ, Ruparel K, Calkins ME, Jackson C, Elliott MA, *et al.* The philadelphia neurodevelopmental cohort: A publicly available resource for the study of normal and abnormal brain development in youth. Neuroimage 2016, 124: 1115–1119.
21. Lisdahl KM, Sher KJ, Conway KP, Gonzalez R, Feldstein Ewing SW, Nixon SJ, *et al.* Adolescent brain cognitive development (ABCD) study: Overview of substance use assessment methods. Dev Cogn Neurosci 2018, 32: 80–96.
22. Schumann G, Loth E, Banaschewski T, Barbot A, Barker G, Büchel C, *et al.* The IMAGEN study: reinforcement-related behaviour in normal brain function and psychopathology. Mol Psychiatry 2010, 15: 1128–1139.
23. Mazziotta J, Toga A, Evans A, Fox P, Lancaster J, Zilles K, *et al.* A probabilistic atlas and reference system for the human brain: International Consortium for Brain Mapping (ICBM). Philos Trans R Soc London Ser B Biol Sci 2001, 356: 1293–1322.

24. Fonov V, Evans AC, Botteron K, Almli CR, McKinstry RC, Collins DL. Unbiased average age-appropriate atlases for pediatric studies. Neuroimage 2011, 54: 313–327.
25. Zhao T, Liao X, Fonov VS, Wang Q, Men W, Wang Y, *et al.* Unbiased age-specific structural brain atlases for Chinese pediatric population. Neuroimage 2019, 189: 55–70.
26. Sanchez CE, Richards JE, Almli CR. Age-Specific MRI Templates for Pediatric Neuroimaging. Dev Neuropsychol 2012, 37: 379–399.
27. Richards JE, Sanchez C, Phillips-Meek M, Xie W. A database of age-appropriate average MRI templates. Neuroimage 2016, 124: 1254–1259.
28. Xie W, Richards JE, Lei D, Zhu H, Lee K, Gong Q. The construction of MRI brain/head templates for Chinese children from 7 to 16 years of age. Dev Cogn Neurosci 2015, 15: 94–105..
29. Yoon U, Fonov VS, Perusse D, Evans AC, Group BDC. The effect of template choice on morphometric analysis of pediatric brain data. Neuroimage 2009, 45: 769–777.
30. Casey BJ, Giedd JN, Thomas KM. Structural and functional brain development and its relation to cognitive development. Biol Psychol 2000, 54: 241–257.
31. Shaw P, Kabani NJ, Lerch JP, Eckstrand K, Lenroot R, Gogtay N, *et al.* Neurodevelopmental trajectories of the human cerebral cortex. J Neurosci 2008, 28: 3586–3594.
32. Rueda MR, Fan J, McCandliss BD, Halparin JD, Gruber DB, Lercari LP, *et al.* Development of attentional networks in childhood. Neuropsychologia 2004, 42: 1029–1040.
33. Konrad K, Neufang S, Thiel CM, Specht K, Hanisch C, Fan J, *et al.* Development of attentional networks: an fMRI study with children and adults. Neuroimage 2005, 28: 429–439.
34. Van Leijenhorst L, Moor BG, de Macks ZAO, Rombouts SARB, Westenberg PM, Crone EA. Adolescent risky decision-making: neurocognitive development of reward and control regions. Neuroimage 2010, 51: 345–355.
35. Ellis CT, Turk-Browne NB. Infant fMRI: a model system for cognitive neuroscience. Trends Cogn Sci 2018, 22: 375–387.
36. De Luca CR, Leventer RJ. Developmental trajectories of executive functions across the lifespan. Psychology Press, 2010, 57–90.
37. Scherf KS, Behrmann M, Humphreys K, Luna B. Visual category-selectivity for faces, places and objects emerges along different developmental trajectories. Dev Sci 2007, 10: F15-30.
38. Zhou Q, Hofer C, Eisenberg N, Reiser M, Spinrad TL, Fabes RA. The developmental trajectories of attention focusing, attentional and behavioral persistence, and externalizing problems during school-age years. Dev Psychol 2007, 43: 369.
39. Meng FC, Xu XJ, Song TJ, Shou XJ, Wang XL, Han SP, *et al.* Development of an autism subtyping questionnaire based on social behaviors. Neurosci Bull 2018, 34: 789–800.
40. Klenberg L, Korkman M, Lahti-Nuuttila P. Differential development of attention and executive functions in 3-to 12-year-old Finnish children. Dev Neuropsychol 2001, 20: 407–428.
41. Geier C, Luna B. The maturation of incentive processing and cognitive control. Pharmacol Biochem Behav 2009, 93: 212–221.
42. Esteban O, Markiewicz CJ, Blair RW, Moodie CA, Isik AI, Erramuzpe A, *et al.* fMRIPrep: a robust preprocessing pipeline for functional MRI. Nat Methods 2019, 16: 111.
43. Fan J, McCandliss BD, Sommer T, Raz A, Posner MI. Testing the efficiency and independence of attentional networks. J Cogn Neurosci 2002, 14: 340–347.
44. Hariri AR, Mattay VS, Tessitore A, Kolachana B, Fera F, Goldman D, *et al.* Serotonin transporter genetic variation and the response of the human amygdala. Science 2002, 297: 400–403.
45. Lejuez CW, Read JP, Kahler CW, Richards JB, Ramsey SE, Stuart GL, *et al.* Evaluation of a behavioral measure of risk taking: the Balloon Analogue Risk Task (BART). J Exp Psychol Appl 2002, 8: 75.
46. Gorgolewski K, Burns CD, Madison C, Clark D, Halchenko YO, Waskom ML, *et al.* Nipype: a flexible, lightweight and extensible neuroimaging data processing framework in python. Front Neuroinform 2011, 5: 13.
47. Johnson MH. Interactive Specialization: A domain-general framework for human functional brain development?. Dev Cogn Neurosci 2011, 1: 7–21.
48. Johnson MH. Functional Brain Development in Infants: Elements of an Interactive Specialization Framework. Child Dev 2000, 71: 75–81.
49. Fan J, Mccandliss B, Fossella J, Flombaum J, Posner M. The activation of attentional networks. Neuroimage 2005, 26: 471–479.
50. Xuan B, Mackie M-A, Spagna A, Wu T, Tian Y, Hof PR, *et al.* The activation of interactive attentional networks. Neuroimage 2016, 129: 308–319.
51. Corbetta M, Shulman GL. Control of goal-directed and stimulus-driven attention in the brain. Nat Rev Neurosci 2002, 3: 201.
52. Raz A, Buhle J. Typologies of attentional networks. Nat Rev Neurosci 2006, 7.
53. Hao L, Sang N, Du X, Qiu J, Wei D, Chen X. Examining brain structures associated with attention networks in a large sample of young adults: a voxel-based morphometry study. Sci Bull 2015, 60: 1824–1832.
54. Paus T. Location and function of the human frontal eye-field: a selective review. Neuropsychologia 1996, 34: 475–483.
55. Casco C, Tressoldi PE, Dellantonio A. Visual selective attention and reading efficiency are related in children. Cortex 1998, 34: 531–546.
56. Lam CM, Beale IL. Relations among sustained attention, reading performance, and teachers' ratings of behavior problems. Remedial Spec Educ 1991, 12: 40–47.
57. Purvis KL, Tannock R. Language abilities in children with attention deficit hyperactivity disorder, reading disabilities, and normal controls. J Abnorm Child Psychol 1997, 25: 133–144.
58. Rabiner D, Coie JD, Group CPPR. Early attention problems and children's reading achievement: A longitudinal investigation. J Am Acad Child Adolesc Psychiatry 2000, 39: 859–867.
59. Facoetti A, Turatto M, Lorusso ML, Mascetti GG. Orienting of visual attention in dyslexia: evidence for asymmetric hemispheric control of attention. Exp Brain Res 2001, 138: 46–53.
60. Harter MR, Anllo-Vento L, Wood FB. Event-related potentials, spatial orienting, and reading disabilities. Psychophysiology 1989, 26: 404–421.
61. Hillen R, Günther T, Kohlen C, Eckers C, van Ermingen-Marbach M, Sass K, *et al.* Identifying brain systems for gaze orienting during reading: fMRI investigation of the Landolt paradigm. Front Hum Neurosci 2013, 7: 384.
62. Anderson P. Assessment and development of executive function (EF) during childhood. Child Neuropsychol 2002, 8: 71–82.
63. Chugani HT. A critical period of brain development: studies of cerebral glucose utilization with PET. Prev Med (Baltim) 1998, 27: 184–188.
64. Kail R. Sources of age differences in speed of processing. Child Dev 1986:969–987.
65. Owen AM, McMillan KM, Laird AR, Bullmore E. N-back working memory paradigm: A meta-analysis of normative functional neuroimaging studies. Hum Brain Mapp 2005, 25:46–59.
66. Blokland GAM, McMahon KL, Hoffman J, Zhu G, Meredith M, Martin NG, *et al.* Quantifying the heritability of task-related brain activation and performance during the N-back working memory task: a twin fMRI study. Biol Psychol 2008, 79: 70–79.

67. Thomas KM, Drevets WC, Whalen PJ, Eccard CH, Dahl RE, Ryan ND, *et al.* Amygdala response to facial expressions in children and adults. Biol Psychiatry 2001, 49: 309–316.
68. Campbell R, Elgar K, Kuntsi J, Akers R, Terstegge J, Coleman M, *et al.* The classification of 'fear'from faces is associated with face recognition skill in women. Neuropsychologia 2002, 40: 575–584.
69. Zahn-Waxler C, Shirtcliff EA, Marceau K. Disorders of childhood and adolescence: Gender and psychopathology. Annu Rev Clin Psychol 2008, 4: 275–303.
70. Rao H, Korczykowski M, Pluta J, Hoang A, Detre JA. Neural correlates of voluntary and involuntary risk taking in the human brain: an fMRI Study of the Balloon Analog Risk Task (BART). Neuroimage 2008, 42: 902–910.
71. Calhoun VD, Wager TD, Krishnan A, Rosch KS, Seymour KE, Nebel MB, *et al.* The impact of T1 versus EPI spatial normalization templates for fMRI data analyses. Hum Brain Mapp 2017, 38: 5331–5342.
72. Gargouri F, Kallel F, Delphine S, Ben Hamida A, Lehéricy S, Valabregue R. The influence of preprocessing steps on graph theory measures derived from resting state fMRI. Front Comput Neurosci 2018, 12: 8.
73. Gavrilescu M, Stuart GW, Rossell S, Henshall K, McKay C, Sergejew AA, *et al.* Functional connectivity estimation in fMRI data: influence of preprocessing and time course selection. Hum Brain Mapp 2008, 29: 1040–1052.
74. Ge Y, Pan Y, Dou W. Analysis of BOLD fMRI signal preprocessing pipeline on different datasets while reducing false positive rates. BIBE 2018, Int Conf Biol Inf Biomed Eng, VDE, 2018, 1–8.
75. Esteban O, Ciric R, Finc K, Blair RW, Markiewicz CJ, Moodie CA, *et al.* Analysis of task-based functional MRI data preprocessed with fMRIPrep. BioRxiv 2019: 694364.
76. Kessler RC, Berglund P, Demler O, Jin R, Merikangas KR, Walters EE. Lifetime prevalence and age-of-onset distributions of DSM-IV disorders in the national comorbidity survey replication. Arch Gen Psychiatry 2005, 62: 593.
77. Kessler RC, Wang PS. The descriptive epidemiology of commonly occurring mental disorders in the united states. Annu Rev Public Health 2008, 29: 115–129.